Vibrational frequencies and spectroscopic constants from quartic force fields for *cis*-HOCO: The radical and the anion

Ryan C. Fortenberry,[1] Xinchuan Huang,[2,a)] Joseph S. Francisco,[3] T. Daniel Crawford,[1,b)] and Timothy J. Lee[4,c)]
[1]*Department of Chemistry, Virginia Tech, Blacksburg, Virginia 24061, USA*
[2]*SETI Institute, 189 Bernardo Avenue, Suite 100, Mountain View, California 94043, USA*
[3]*Department of Chemistry, Purdue University, West Lafayette, Indiana 47907, USA*
[4]*NASA Ames Research Center, Moffett Field, California 94035-1000, USA*

(Received 21 October 2011; accepted 2 November 2011; published online 2 December 2011)

The use of accurate quartic force fields together with vibrational configuration interaction recently predicted gas phase fundamental vibrational frequencies of the *trans*-HOCO radical to within 4 cm^{-1} of experimental results for the two highest frequency modes. Utilizing the same approach, we are providing a full list of fundamental vibrational frequencies and spectroscopic constants for the *cis*-HOCO system in both radical and anionic forms. Our predicted geometrical parameters of the *cis*-HOCO radical match experiment and previous computation to better than 1% deviation, and previous theoretical work agrees equally well for the anion. Correspondence between vibrational perturbation theory and variational vibrational configuration interaction for prediction of the frequencies of each mode is strong, better than 5 cm^{-1}, except for the torsional motion, similar to what has been previously identified in the *trans*-HOCO radical. Among other considerations, our results are immediately applicable to dissociative photodetachment experiments which initially draw on the *cis*-HOCO anion since it is the most stable conformer of the anion and is used to gain insight into the portion of the OH + CO potential surface where the HOCO radical is believed to form, and we are also providing highly accurate electron binding energies relevant to these experiments. © *2011 American Institute of Physics*. [doi:10.1063/1.3663615]

I. INTRODUCTION

For many years now, dissociative photodetachment (DPD) techniques carried out on the $HOCO^-$ molecular anion[1–4] have been used to study various aspects of potential energy surfaces involving OH + CO. The hydroxyformyl (HOCO) radical is hypothesized to be an intermediate species in the reaction of these two small molecules,[5,6] and its experimental study is most easily initiated by photodetachment of the more stable anion.[1] The pressure dependence and strong isotopic effect for deuterium substitution of the hydroxy radical in the OH + CO reaction rate give some indication that the chemistry of this system does not proceed directly to the creation of CO_2 and the other established products, mainly hydrogen.[7] Instead, it is believed that HOCO is created and then breaks down into CO_2 and H. If confirmation of this pathway is fully established, better understanding of the associated chemistry would yield deeper insights into the atmospheric processes not only of the Earth[8,9] but potentially even Mars,[10,11] where the atmospheric chemistry is dominated by CO_2.[11,12]

As *cis*-$HOCO^-$ is the most stable anionic conformer, it is the one most likely to be created for subsequent use in the DPD experiments.[1] Photodetachment results in the *cis*-HOCO radical plus e^- complex which goes through a barrier of about 10 kcal/mol to produce the more stable *trans*-HOCO radical conformer after the removal of the electron from the system.[13] From there, the continuance of the OH + CO potential surface may be studied as HOCO progresses along the reaction coordinate to give CO_2 and hydrogen. A full understanding of these processes, however, cannot be clearly elucidated until the molecular species in question can be observed. The greatest hope of this has been through infrared spectroscopy, but only the O−H and C=O stretching fundamental vibrational frequencies have been conclusively recorded in the gas phase and only for the more stable *trans* conformer of the radical.[14,15] There does exist condensed phase (in matrices of Ne, Ar, and CO) fundamental vibrational frequency data for all six fundamentals of the *trans* conformer[5,16,17] and CO matrix condensed phase data for all fundamentals except the torsional mode of the *cis* conformer,[5] but it is unclear how the condensed phase numbers would relate to the necessary gas phase observations applicable to atmospheric studies of either Earth or Mars.

Very recently, we utilized *ab initio* quantum chemical computations and quartic force fields (QFFs) to predict the gas phase fundamental vibrational frequencies of the *trans*-HOCO radical.[18] For the two known fundamental frequencies, our theoretical results match experiment to within 5 cm^{-1}, and there is no indication that any of the other frequencies predicted for the rest of the fundamentals should be any less accurate since we used established techniques calibrated to produce such high quality results for other

a)Electronic mail: Xinchuan.Huang-1@nasa.gov.
b)Electronic mail: crawdad@vt.edu.
c)Electronic mail: Timothy.J.Lee@nasa.gov.

molecular systems.[19–23] As mentioned above, there is no known gas phase measurement or prediction of the fundamental vibrational frequencies of the *cis*-HOCO radical or of the *cis*-$HOCO^-$ molecular anion. In this paper, we will utilize the same techniques applied previously to the *trans*-HOCO radical[18] to predict accurately the fundamental vibrational frequencies for infrared observation and the associated spectroscopic constants useful for rotational or rovibrational spectroscopy for both the *cis*-HOCO radical and the *cis*-HOCO anion.

II. COMPUTATIONAL DETAILS

Coupled cluster theory is one of the most accurate quantum chemical approaches known to date,[24–26] and its use in the computation of energy points on a potential surface necessary for the creation of a quartic force field has been well established.[18–23,27] As with many of these previous studies, the work presented here makes exclusive use of the coupled cluster singles, doubles, and perturbative triples [CCSD(T)] (Ref. 28) level of theory which is often called the "gold standard" of quantum chemistry.[26] Computations of the *cis*-HOCO radical are based on restricted open-shell Hartree Fock (ROHF) (Ref. 29) reference wavefunctions, while spin restricted Hartree Fock (RHF) (Refs. 30 and 31) references are utilized for the closed-shell anion. Geometry optimizations of the equilibrium structures are based on CCSD(T) computations utilizing the aug-cc-pV5Z basis set.[32–34] The geometry is then compositely modified to include corrections for core-correlation effects based on basis sets specifically developed for this purpose by Martin and Taylor[35] which we shall call the MT basis sets.

The QFFs for both of the C_s symmetry molecular species of interest are made up of 743 symmetry unique points. These are determined by displacements of 0.005 Å for each of the bond lengths (from Fig. 1: C = O_2 which is internal coordinate 1; C−O_1, coordinate 2; and O_1−H, coordinate 3) and 0.005 radians for each bond angle (O_1−C−O_2 defined as coordinate 4 and H−O_1−C, coordinate 5) as well as the torsional mode which is internal coordinate 6. At each point CCSD(T) computations with aug-cc-pVXZ for X = T, Q, and 5 are carried out. The resulting energies are then extrapolated out to the complete basis set (CBS) limit via an established three-point formula.[36] Subsequent corrections to this energy can be made for core correlation effects using the aforementioned MT basis set[35] and scalar relativistic effects established by Douglas and Kroll[37] with the aug-cc-pVTZ basis set which we will refer to as aTZ-DK. Differently from previous studies,[18,21,22,38] higher order electron correlation effects are not included in the QFFs for this study because neither the averaged coupled pair functional (ACPF) method[21,22,38] nor full CCSDT[18] have been shown to properly treat this correction. The total composite energy computed for each point is thus defined as

$$E_{tot} = E_{\mathrm{aTQ5}\rightarrow\mathrm{CBS}} + (E_{\mathrm{MT,core}} - E_{\mathrm{MT}}) + (E_{\mathrm{aTZ-DK,rel.}} - E_{\mathrm{aTZ-DK}}). \quad (1)$$

The QFF defined by composite energies inclusive of each correction listed will be referred to as the CcCR QFF as it includes the extrapolated CBS energy, core Correlation effects, and Relativistic terms. We also make use of the less descriptive CR QFF where the core correlation term is neglected. These two QFFs have previously predicted highly accurate fundamental vibrational frequencies and spectroscopic constants for the *trans*-HOCO radical.[18] All electronic structure computations are undertaken with the MOLPRO 2010.1 program.[39]

The simple internal force constants and the actual equilibrium geometry for a QFF are determined from our accurate least-squares fits where the sum of the residuals squared (in units of $a.u.^2$) is on the order of less than 10^{-16}. Cartesian derivatives are computed from the internal coordinate force constants by the INTDER program,[40] and second-order vibrational perturbation theory (VPT) (Refs. 41–43) in the SPECTRO program[44] is utilized for prediction of the fundamentals and spectroscopic constants. Additionally, a Morse-cosine transformation of the force constants leads to realistic dissociation limits and periodic torsional potential functions[19] which allows for the use of the vibrational configuration interaction (VCI) method implemented in the MULTIMODE program[45,46] to further elucidate the gas phase fundamental vibrational frequencies.

III. RESULTS

The CcCR QFF geometries of the *cis*-HOCO radical and anion are shown in Figs. 1(a) and 1(b) and are quantitatively described in Tables I and II. Previous work on the *trans*-HOCO radical conformer[18] utilized the additional higher order electron correlation term to describe the geometry. This QFF matched experimentally derived and other accurately computed geometrical parameters very closely. However, the enhanced cost of the CcCRE QFF and the little difference between its prediction of the *trans*-HOCO equilibrium

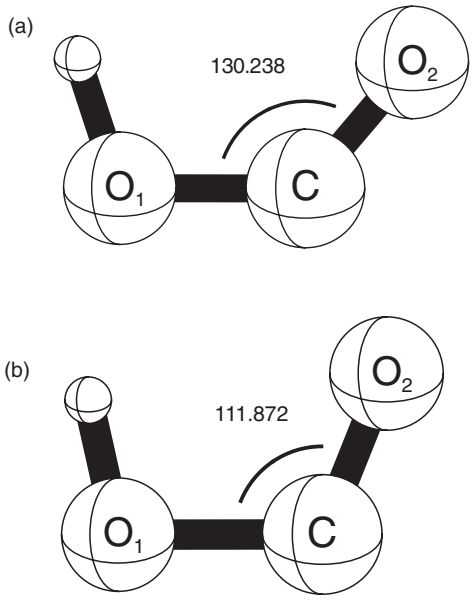

FIG. 1. The equilibrium geometry of the *cis*-HOCO radical (a) and anion (b) both computed from the CcCR QFF. The O_1−C−O_2 bond angles are both given to highlight the change in this parameter. All other geometric values can be found in Table I for the radical and Table II for the anion.

TABLE I. The *cis*-HOCO minimum structure, rotational constants, and harmonic frequencies from the more descriptive CcCR QFF defined in Eq. (1).

Zero-point			Equilibrium			
	This work	Experiment[a]		This work	Oyama *et al.*[b]	Botschwina[c]
$R(O_1-H)$	0.970 85 Å	0.991 Å	$R(O_1-H)$	0.970 91 Å	0.972 Å	0.9711 Å
$R(C-O_1)$	1.333 16 Å	1.329 Å	$R(C-O_1)$	1.325 97 Å	1.329 Å	1.3275 Å
$R(C-O_2)$	1.183 19 Å	1.184 Å	$R(C-O_2)$	1.180 37 Å	1.183 Å	1.1811 Å
$\angle H-O_1-C$	108.859°	108.0°	$\angle H-O_1-C$	108.210°	108.1°	108.07°
$\angle O_1-C-O_2$	130.437°	130.3°	$\angle O_1-C-O_2$	130.238°	130.2°	130.33°
A_0	4.775 03 cm^{-1}	4.768 13 cm^{-1}	A_e	4.733 17 cm^{-1}	...	4.739 0 cm^{-1}
B_0	0.392 18 cm^{-1}	0.391 59 cm^{-1}	B_e	0.395 49 cm^{-1}	...	0.394 51 cm^{-1}
C_0	0.361 80 cm^{-1}	0.361 25 cm^{-1}	C_e	0.364 99 cm^{-1}	...	0.364 19 cm^{-1}

Mode	Description	Freq (in cm^{-1})
ω_1	a′ O_1-H stretch	3662.0
ω_2	a′ $C=O_2$ stretch	1864.9
ω_3	a′ $H-O_1-C$ bend	1313.9
ω_4	a′ $C-O_1$ stretch	1084.1
ω_5	a′ O_1-C-O_2 bend	607.4
ω_6	a″ torsional mode	578.4

[a]Fourier-transformed microwave results from Ref. 47.
[b]UCCSD(T)-F12/aug-cc-pVTZ results from Ref. 47.
[c]RCCSD(T)/cc-pCVQZ results Ref. 48.

geometry and that of the CcCR geometry (a change of less than 0.001 Å and 0.1°) with the additional similarity between the fundamental frequencies of the CcCRE and CcCR QFFs (Ref. 18) has led us to utilize the CcCR QFF as the basis for this present study of the *cis*-HOCO radical and anion. From this, however, we can still make comparison between the geometries of the *cis*- and *trans*-HOCO radicals. The O_1-H bond is about 0.015 Å shorter in the *trans* conformer, while the distance between the C and O_1 atoms is shorter by about the same margin in the *cis*. The $R(C-O_2)$ variable differs by less than 0.005 Å between the two conformers. The $H-O_1-C$ bond angles are nearly identical for the two geometrical conformations of the HOCO radical while the O_1-C-O_2 angle is about 3.5° wider for the *cis* radical. From the CcCR QFF minima, the *trans*-HOCO conformer[18] is 1.8 kcal/mol lower in energy than the *cis* conformer which is exactly in agreement with previous work.[7] Additionally, ROHF-CCSD/aug-cc-pVTZ computations of displacements along the torsional coordinate set the barrier to a near 90° rotation from the *trans* conformer at 27.3 kcal/mol and 23.6 kcal/mol from the *cis*-HOCO radical conformer also in close agreement with previous work.[7]

TABLE II. The minimum structure, rotational constants, and harmonic frequencies for *cis*-$HOCO^-$ as computed from the CcCR QFF defined in Eq. (1).

Zero-point		Equilibrium		
	This work		This work	Dixon *et al.*[a]
$R(O_1-H)$	0.976 40 Å	$R(O_1-H)$	0.975 91 Å	0.980 Å
$R(C-O_1)$	1.463 42 Å	$R(C-O_1)$	1.444 60 Å	1.458 Å
$R(C-O_2)$	1.227 81 Å	$R(C-O_2)$	1.226 70 Å	1.235 Å
$\angle H-O_1-C$	103.116°	$\angle H-O_1-C$	102.537°	102.3°
$\angle O_1-C-O_2$	112.062°	$\angle O_1-C-O_2$	111.872°	111.8°
A_0	2.824 57 cm^{-1}	A_e	2.825 21 cm^{-1}	...
B_0	0.412 41 cm^{-1}	B_e	0.419 18 cm^{-1}	...
C_0	0.359 07 cm^{-1}	C_e	0.365 02 cm^{-1}	...

		Freq (in cm^{-1})	
Mode	Description	This work	Dixon *et al.*[b]
ω_1	a′ O_1-H stretch	3540.5	3514
ω_2	a′ $C=O_2$ stretch	1588.3	1551
ω_3	a′ $H-O_1-C$ bend	1202.4	1170
ω_4	a′ $C-O_1$ stretch	718.4	661
ω_5	a′ O_1-C-O_2 bend	580.5	510
ω_6	a″ torsional mode	655.8	624

[a]CCSD(T)/aug-cc-pVTZ prediction from Ref. 49.
[b]CCSD(T)/aug-cc-pVDZ prediction from Ref. 49.

TABLE III. CcCR (from Eq. (1)) and CR (which neglects the core correlation in Eq. (1)) QFF fundamental vibrational frequencies (in cm^{-1}) for the *cis*-HOCO radical from VPT and VCI computations as well as condensed phase experimental results.

Mode	Description	CcCR		CR		Experiment[a]	Previous theory[b]
		VPT	VCI	VPT	VCI		
ν_1	a′ O_1-H stretch	3450.8	3452.3	3446.1	3447.5	3316	3587
ν_2	a′ $C=O_2$ stretch	1823.4	1824.1	1816.6	1817.0	1797	1836
ν_3	a′ $H-O_1-C$ bend	1284.4	1280.2	1282.7	1278.7	1261	1161
ν_4	a′ $C-O_1$ stretch	1045.9	1042.4	1040.3	1037.7	1088	1010
ν_5	a′ O_1-C-O_2 bend	601.7	601.2	598.8	598.3	620	547
ν_6	a″ torsional mode	566.5	540.2	564.2	538.1		413
ZPE		4491.4	4485.7	4479.0	4473.2		4383

[a]Condensed phase data in a CO matrix from Milligan and Jacox (Ref. 5).
[b]4MR VCI result from Bowman, Christoffel, and Weinberg (Ref. 50).

Agreement between geometries lessens with the inclusion of an additional electron to the system even for molecules with the same dihedral angle. The most striking difference between the CcCR geometries of the *cis*-HOCO radical and *cis*-HOCO anion is in the O_1-C-O_2 bond angle. The difference of roughly 20° results from a decrease in the angle from 130.2° for the radical to 111.9° in the anion. In the anion, HOCO is substantially less linear in structure, as is evidenced by the small O_1-C-O_2 bond angle, and the reduced bond angle brings about a smaller *A* rotational constant. This rotational constant is nearly halved with the addition of the electron to the molecular system. The *B* rotational constant is increased slightly for the anion with respect to the radical while the *C* constant differs little between the two molecules. Additionally, the $H-O_1-C$ bond angle is smaller for the anion than the radical, and all of the bond lengths are longer in the anion than they are in the radical, which is expected. Increased correlation effects due to the presence of the extra electron in the anion lead to longer bond lengths. Additionally, the extra electron also increases the interaction between the terminal oxygen atom (O_2) and the hydrogen. The interaction of the terminal atoms more easily creates a resonance in the anion than in the radical and, subsequently, decreases the O_1-C-O_2 bond angle enough such that a more cyclic structure results where the hydrogen atom or merely a proton may be viewed as migrating between the two oxygen atoms.

Our geometries for the two structures are very close (within 0.5%) to previous theoretical predictions (Refs. 47 and 48 for the radical and Ref. 49 for the anion), and the geometrical parameters for the radical vary little from experimental results[47] since our data are within 0.9%. The one exception is the O_1-H bond distance of the radical where experiment pins this value at 0.02 Å longer than our predictions, but the theoretical results both from within the same study as well as other previous work[48] appear to indicate that some chronic difference between theory and experiment is present for this value. As a further note, the experimental value for the O_1-H bond length for the *trans* conformer is greater than our predicted value[18] also by about 0.02 Å.

The removal of the core correlation component of the QFF affects the geometry little but still noticeably for both the radical and the anion. For the *cis*-HOCO radical, use of the CR QFF as opposed to the CcCR QFF results in an O_1-H bond length that is 0.0008 Å longer, a $C-O_1$ bond length 0.003 Å longer, and a $C-O_2$ bond length that is 0.002 Å longer. The $H-O_1-C$ bond angle decreases to 131.2° and the O_1-C-O_2 to 108.1°, changes of less than 0.2°. For the anion, each of the equilibrium bond lengths increases by no more than 0.005 Å when shifting from the CcCR QFF to the CR. Conversely, both of the bond angles decrease by less than 0.1°. Hence, the CR QFF predicts longer bond lengths than the CcCR QFF across the board while also decreasing the bond angles. Even though these changes are not substantial, computation of highly accurate geometries is vital in the prediction of accurate fundamental vibrational frequencies and spectroscopic constants, and an understanding of these differences in the geometries predicted by the two QFFs is subsequently necessary.

Besides the geometric parameters, Tables I and II also list the CcCR harmonic vibrational frequencies for the *cis*-HOCO radical and anion, respectively. The anharmonic frequencies are quantitatively described in Tables III and IV; the anharmonic constant matrices for both forms of HOCO analyzed in this work are given in Tables V and VI. The CcCR quadratic, cubic, and quartic force constants are listed in Tables VII and VIII, and the spectroscopic constants for both the radical and the anion are all inventoried in Table IX.

TABLE IV. Fundamental vibrational frequencies (in cm^{-1}) for $HOCO^-$ in the lowest energy *cis* conformation from the CcCR and CR QFF VPT and VCI computations.

Mode	Description	CcCR		CR	
		VPT	VCI	VPT	VCI
ν_1	a′ O_1-H stretch	3306.4	3306.5	3306.2	3304.7
ν_2	a′ $C=O_2$ stretch	1569.4	1565.2	1563.2	1558.0
ν_3	a′ $H-O_1-C$ bend	1128.1	1125.0	1119.3	1115.1
ν_4	a′ $C-O_1$ stretch	669.8	669.9	666.5	666.4
ν_5	a′ O_1-C-O_2 bend	526.4	524.6	518.2	516.0
ν_6	a″ torsional mode	612.5	598.0	605.1	590.6
ZPE		4066.7	4058.6	4052.1	4044.0

TABLE V. CcCR QFF anharmonic constant matrix (in cm^{-1}) for the *cis*-HOCO radical.

Mode	1	2	3	4	5	6
1	−99.114					
2	1.967	−13.319				
3	−24.593	−5.222	−7.365			
4	−2.419	−13.192	−17.725	−7.551		
5	−3.937	−6.313	−2.656	−5.763	0.674	
6	3.013	−0.470	−11.111	−6.599	4.583	−3.142

A. Fundamental frequencies of the *cis*-HOCO radical

Since no gas phase experimental data exists for the fundamental vibrational frequencies of the $X\,^2A'$ *cis*-HOCO radical, our computed values given in Table III are a necessary complete set of highly accurate fundamental frequencies provided for this system. Bowman *et al.*[50] have previously computed fundamental vibrational frequencies of the *cis*- and *trans*-HOCO radicals with an earlier version of the MULTIMODE program[45] from a lower-level CISD/DZP potential surface formulated by Schatz *et al.*[51] Our results and those from Ref. 50 do not demonstrate strong agreement as those computed previously could not benefit from more advanced computational methods, basis sets, and composite approaches. Even though, condensed phase frequencies obtained from the use of CO matrices have also been reported,[5] the torsional motion (ν_6) could not be obtained in this experiment. Additionally, it is unclear how the condensed phase frequencies compare to their gas phase counterparts because the magnitude of the matrix perturbations have not been quantified. Our predictions for the O_1-H stretch (ν_1), $C=O_2$ stretch (ν_2), and the $H-O_1-C$ angle bend (ν_3) indicate that the condensed phase results have a lower frequency than these same modes in the gas phase. Conversely, our predictions of the gas phase $C-O_1$ (ν_4) stretch and O_1-C-O_2 (ν_5) bond angle bend have frequencies as much as 50 cm^{-1} lower than the corresponding modes from the condensed phase experiment. However, since we are utilizing the exact procedure as was previously executed for the *trans*-HOCO radical,[18] we should be able to assume that our predicted gas phase fundamental vibrational frequencies for the *cis*-HOCO radical are similarly accurate: within 5 cm^{-1} or, often, better.

In Table III, the fundamental frequencies are listed for each mode computed with both the CcCR and CR QFFs making use of both VPT and VCI. All of our reported VCI results are from computations utilizing 5-mode representations as discussed previously.[18,23,46] The difference between the 4-mode coupling and the 5-mode coupling is on the order of less than 0.5 cm^{-1} indicating that convergence of the mode coupling is achieved. For the convergence of the vibrational variational basis functions used in VCI, all modes actually converge for a set of basis functions at 15 428 functions for the a' matrix in this C_s molecule and 9981 functions for a". The one exception to this is the ν_4 mode which requires more functions in order for it to be fully described: 21 583 for the a' matrix and 14 141 for a". Subsequently, on the final VCI computations, 31 primitive harmonic oscillator basis functions contracted down to 14 actual bases are required for each mode with 20 Gauss-Hermite (HEG) quadrature points also included in the computation. VPT, on the other hand, requires the inclusion of a fourfold Fermi resonance polyad[52] explicitly for ν_3, ν_4, $2\nu_5$, and $2\nu_6$. Two type-2 Fermi resonances are included for $\nu_5+\nu_3=\nu_2$ and $\nu_5+\nu_4=\nu_2$, while a Coriolis resonance for ν_5 and ν_6 is also required in the computation.

The earlier computations by Bowman *et al.*[50] are quite different from those we are presenting here. The previous study made use of 4MR computations with 4501 basis functions. The potential surface employed in this study was built with a diatom-diatom grid of OH–CO Jacobi coordinates which allowed for better descriptions of the reaction coordinates.[51] However, the quality of these descriptions actually decreases in the region around the minimum further impeding the quality of the computation. Additionally, the lower level nature of the method and basis set used in the computation of the potential energy surface also hindered the accuracies of the reported frequencies. This is most clearly evidenced in the difference in frequencies between our ν_6 mode and those reported earlier; the difference is on the order of 125 cm^{-1}.

The level of agreement in this present study between the frequencies predicted by VPT and VCI (listed in Table III) for the *cis*-HOCO radical is quite good. The ν_2 and ν_5 modes differ by less than 1 cm^{-1} for both the CcCR and CR QFFs, while ν_1, ν_3, and ν_4 differ between VPT and VCI by less than 5 cm^{-1}. The level of agreement for ν_5, the O_1-C-O_2 bend, is exceptionally good. For both QFFs, VPT predicts frequencies just 0.5 cm^{-1} higher than VCI, and the difference in energy between the two QFFs for ν_5 is at about 3 cm^{-1}. Furthermore, the zero-point energies (ZPEs) for both QFFs are within 6 cm^{-1} of one another for the different computational approaches. Conversely, the CcCR VPT ν_6 of 566.5 cm^{-1} and VCI ν_6 of 540.2 cm^{-1} differ by 26.3 cm^{-1}. The CR ν_6 difference is comparable. Similar behavior was present previously in the *trans*-HOCO radical.[18] Hence, this large difference between VPT and VCI for ν_6 is not unexpected. The VCI probably does a better job of fully describing the anharmonicity than VPT since it fully allows for the various modes to couple to one another in the bases, but only explicitly including the torsional coordinate would finally resolve the discrepancy.

The difference in frequencies between the QFFs is not significant. Even ν_6 exhibits insubstantial change for the choice of QFF, and the ν_5 mode, which has the smallest VPT/VCI difference, is typical in this regard as most modes only differ between QFFs by about the same 3 cm^{-1} margin

TABLE VI. *cis*-$HOCO^-$ CcCR QFF anharmonic constant matrix (in cm^{-1}).

Mode	1	2	3	4	5	6
1	−117.943					
2	−4.208	−12.020				
3	−21.622	−2.581	−10.619			
4	3.587	7.560	−18.500	−14.197		
5	10.967	5.113	−19.982	−31.927	−10.352	
6	14.897	4.307	−10.476	−17.173	−14.731	−15.854

TABLE VII. The CcCR QFF quadratic, cubic, and quartic force constants (in mdyn/Å$^n \cdot$rad^m) of the *cis*-HOCO radical in the simple-internal coordinate system.

F_{11}	14.179 761	F_{431}	0.3018	F_{1111}	575.80	F_{4432}	0.47	F_{5531}	−0.55
F_{21}	1.383 182	F_{432}	0.6831	F_{2111}	7.88	F_{4433}	−1.24	F_{5532}	0.71
F_{22}	6.142 490	F_{433}	−0.2551	F_{2211}	−1.45	F_{4441}	2.76	F_{5533}	−0.61
F_{31}	0.000 591	F_{441}	−1.7343	F_{2221}	8.05	F_{4442}	6.00	F_{5541}	0.61
F_{32}	0.267 404	F_{442}	−1.8680	F_{2222}	246.57	F_{4443}	−0.65	F_{5542}	0.08
F_{33}	7.520 275	F_{443}	−0.0909	F_{3111}	1.17	F_{4444}	4.39	F_{5543}	−0.15
F_{41}	0.437 598	F_{444}	−1.6304	F_{3211}	0.66	F_{5111}	−0.48	F_{5544}	0.84
F_{42}	0.370 888	F_{511}	−0.1197	F_{3221}	0.24	F_{5211}	−0.60	F_{5551}	1.06
F_{43}	−0.181 404	F_{521}	0.1691	F_{3222}	9.61	F_{5221}	0.18	F_{5552}	1.14
F_{44}	1.360 927	F_{522}	−0.6451	F_{3311}	−0.75	F_{5222}	−0.08	F_{5553}	0.73
F_{51}	−0.010 299	F_{531}	0.0918	F_{3321}	−1.04	F_{5311}	−0.34	F_{5554}	0.67
F_{52}	0.388 361	F_{532}	−0.5804	F_{3322}	−5.31	F_{5321}	0.19	F_{5555}	−0.25
F_{53}	0.180 206	F_{533}	−0.1368	F_{3331}	0.72	F_{5322}	1.25	F_{6611}	−0.09
F_{54}	−0.151 470	F_{541}	0.0413	F_{3332}	2.29	F_{5331}	−0.37	F_{6621}	0.19
F_{55}	0.741 796	F_{542}	−0.0760	F_{3333}	334.60	F_{5332}	−0.12	F_{6622}	0.68
F_{66}	0.108 268	F_{543}	0.0224	F_{4111}	2.77	F_{5333}	−1.47	F_{6631}	−0.22
F_{111}	−100.7780	F_{544}	−0.1614	F_{4211}	3.67	F_{5411}	0.61	F_{6632}	−0.19
F_{211}	−3.6110	F_{551}	−0.1348	F_{4221}	6.39	F_{5421}	0.47	F_{6633}	0.30
F_{221}	−0.8647	F_{552}	−0.6373	F_{4222}	4.31	F_{5422}	0.82	F_{6641}	−0.13
F_{222}	−45.7350	F_{553}	−0.3061	F_{4311}	−0.57	F_{5431}	−0.15	F_{6642}	0.27
F_{311}	−0.3016	F_{554}	−0.0224	F_{4321}	−1.48	F_{5432}	−0.07	F_{6643}	0.00
F_{321}	−0.0540	F_{555}	−1.0132	F_{4322}	−2.80	F_{5433}	−0.49	F_{6644}	0.31
F_{322}	−2.0350	F_{661}	0.0411	F_{4331}	0.65	F_{5441}	0.17	F_{6651}	−0.03
F_{331}	0.3751	F_{662}	−0.3076	F_{4332}	1.87	F_{5442}	0.69	F_{6652}	0.21
F_{332}	1.0000	F_{663}	0.0482	F_{4333}	−1.52	F_{5443}	−0.87	F_{6653}	−0.02
F_{333}	−54.5168	F_{664}	−0.0452	F_{4411}	−0.75	F_{5444}	0.98	F_{6654}	0.19
F_{411}	−0.7347	F_{665}	−0.0703	F_{4421}	3.44	F_{5511}	−0.23	F_{6655}	−0.06
F_{421}	−1.4412			F_{4422}	1.15	F_{5521}	1.19	F_{6666}	−0.13
F_{422}	−1.9267			F_{4431}	0.66	F_{5522}	0.08		

mentioned above. The one exception to this is ν_2, but its frequency varies from the CcCR to CR QFF by 6.8 cm^{-1} for VPT and 7.1 cm^{-1} for VCI, a small percentage change in this frequency range. Such behavior is expected. Core correlation for the C=O$_2$ bond should be greater than for other modes since this double bonded moiety is more susceptible to the effects of core correlation. Inclusion of this factor typically gives even tighter bonds and, subsequently, higher frequencies than computations without core correlation. Besides the expected difference between VPT and VCI for ν_6, the consistency check between the two computational approaches, the fairly close agreement for the individual frequencies between QFFs, and the presence of similar behavior in the torsional motion between the VPT and VCI frequencies as predicted in our previous study on the *trans*-HOCO radical,[18] all indicate that our prediction of these fundamental vibrational frequencies is very close to the true, physical values.

B. Fundamental frequencies of the *cis*-HOCO$^-$ anion

The computations of the fundamental frequencies of the $X\,^1A'$ *cis*-HOCO anion differ somewhat from their radical counterparts. First and most noticeably, the ordering of the fundamentals changes for both the harmonic (Table II) and the anharmonic (Table IV) frequencies. The torsional motion (ν_6) is more energetic, while the O$_1$−C−O$_2$ bond (ν_5) is less so as a result of the decrease in the O$_1$−C−O$_2$ bond angle compared to the radical. Next, the number of basis functions necessary to converge the system is less than that required of the radical: 11 820 for the a' matrix and 6 115 for a". The number of functions required for convergence must be increased on the ν_3 and ν_6 modes in the anion, whereas ν_4 necessitates this for the radical. In the anion, there are again 31 primitive harmonic oscillator functions used for each mode, but these are contracted down to 21 vibrational variational basis functions with 26 HEG points required of the anion for the ν_6 mode. Nineteen contracted functions and 24 HEG points are utilized for ν_3, while all of the other modes only require 13 contracted functions and 18 HEG points. Lastly, the VPT computations have different Fermi resonance polyads[52] as they are made up of ν_2, $2\nu_4$, $2\nu_5$, $2\nu_6$, $\nu_3 + \nu_5$, and $\nu_4 + \nu_5$; a type-2 Fermi resonance, $\nu_5 + \nu_4 = \nu_3$; and two Coriolis resonances with the first for ν_6 and ν_4 and the second for ν_5 and ν_4. However, these required resonances do have many similarities with the *cis* radical. Like the radical computations, on the other hand, the mode representation coupling in the VCI computations converges for the use of a 5-mode representation which is utilized in the predictions of all fundamental vibrational frequencies with VCI.

Compared to the previous *trans*-HOCO radical work and other molecules we have recently studied,[18,21–23] the *cis*-HOCO anion is unique in the VPT analysis as it requires the inclusion of a special type of resonance between ν_4 and ν_5. Regular Fermi type 1 and 2 resonances involve overtones

TABLE VIII. The *cis*-$HOCO^-$ CcCR QFF quadratic, cubic, and quartic force constants (in mdyn/$Å^n \cdot rad^m$) in the simple-internal coordinate system.

F_{11}	10.622 693	F_{431}	0.5490	F_{1111}	430.20	F_{4432}	0.90	F_{5531}	−1.09
F_{21}	1.602 313	F_{432}	0.6751	F_{2111}	8.25	F_{4433}	−1.74	F_{5532}	1.77
F_{22}	2.265 812	F_{433}	−0.1963	F_{2211}	3.44	F_{4441}	8.10	F_{5533}	−2.22
F_{31}	0.037 188	F_{441}	−2.3356	F_{2221}	5.77	F_{4442}	11.38	F_{5541}	0.78
F_{32}	0.429 239	F_{442}	−2.6537	F_{2222}	149.29	F_{4443}	−1.15	F_{5542}	−0.03
F_{33}	7.032 887	F_{443}	−0.0420	F_{3111}	0.32	F_{4444}	16.16	F_{5543}	0.57
F_{41}	0.963 369	F_{444}	−4.8742	F_{3211}	−0.75	F_{5111}	0.32	F_{5544}	0.71
F_{42}	0.618 000	F_{511}	−0.1905	F_{3221}	−1.41	F_{5211}	0.38	F_{5551}	1.57
F_{43}	−0.282 887	F_{521}	0.0228	F_{3222}	6.31	F_{5221}	1.43	F_{5552}	1.35
F_{44}	2.037 157	F_{522}	−0.7824	F_{3311}	−0.42	F_{5222}	2.08	F_{5553}	0.85
F_{51}	0.061 125	F_{531}	0.4314	F_{3321}	−0.45	F_{5311}	−0.80	F_{5554}	0.93
F_{52}	0.154 799	F_{532}	−0.7714	F_{3322}	−5.13	F_{5321}	−0.32	F_{5555}	0.75
F_{53}	0.120 421	F_{533}	0.0975	F_{3331}	0.13	F_{5322}	2.76	F_{6611}	−0.51
F_{54}	–0.209 791	F_{541}	−0.3518	F_{3332}	1.41	F_{5331}	−0.37	F_{6621}	−0.22
F_{55}	0.681 612	F_{542}	−0.0503	F_{3333}	325.99	F_{5332}	−1.00	F_{6622}	1.07
F_{66}	0.178 223	F_{543}	−0.2151	F_{4111}	−0.54	F_{5333}	−0.98	F_{6631}	0.13
F_{111}	−74.0150	F_{544}	−0.1974	F_{4211}	7.59	F_{5411}	1.06	F_{6632}	−0.62
F_{211}	−4.3343	F_{551}	−0.2101	F_{4221}	7.75	F_{5421}	0.93	F_{6633}	0.31
F_{221}	−1.0178	F_{552}	−1.2712	F_{4222}	5.53	F_{5422}	0.75	F_{6641}	−0.41
F_{222}	−21.9473	F_{553}	−0.3912	F_{4311}	0.57	F_{5431}	−0.94	F_{6642}	0.44
F_{311}	−0.1220	F_{554}	−0.1299	F_{4321}	−1.67	F_{5432}	1.28	F_{6643}	−0.20
F_{321}	0.1644	F_{555}	−0.9958	F_{4322}	−1.01	F_{5433}	−1.52	F_{6644}	−0.06
F_{322}	−1.8350	F_{661}	0.1646	F_{4331}	0.27	F_{5441}	0.92	F_{6651}	−0.20
F_{331}	0.3642	F_{662}	−0.4663	F_{4332}	0.79	F_{5442}	1.10	F_{6652}	0.42
F_{332}	1.3229	F_{663}	0.1761	F_{4333}	−1.60	F_{5443}	−0.05	F_{6653}	−0.26
F_{333}	−52.9280	F_{664}	−0.1225	F_{4411}	−1.93	F_{5444}	1.98	F_{6654}	0.39
F_{411}	−2.1495	F_{665}	−0.1133	F_{4421}	6.10	F_{5511}	0.19	F_{6655}	−0.11
F_{421}	−3.1007			F_{4422}	1.55	F_{5521}	1.81	F_{6666}	−0.79
F_{422}	−3.1187			F_{4431}	−0.88	F_{5522}	0.56		

TABLE IX. CcCR QFF computed vibration-rotation interaction constants and quartic and sextic centrifugal distortion constants of the *cis*-HOCO radical and anion.

	Vib-Rot constants (MHz)				Distortion constants				Watson *S* reduction			
	Mode	α^A	α^B	α^C	(MHz)			(Hz)	(MHz)			(Hz)
cis-HOCO	1	405.2	3.9	4.9	τ'_{aaaa}	−52.552	Φ_{aaa}	3927.342	D_J	0.010	H_J	0.013
radical	2	1369.6	48.6	44.0	τ'_{bbbb}	−0.051	Φ_{bbb}	0.025	D_{JK}	−0.296	H_{JK}	−0.618
	3	−2422.0	14.6	31.3	τ'_{cccc}	−0.029	Φ_{ccc}	0.003	D_K	13.424	H_{KJ}	−105.557
	4	−572.1	77.8	86.0	τ'_{aabb}	0.622	Φ_{aab}	−51.657	d_1	−0.001	H_K	4033.504
	5	−2863.0	−5.0	13.8	τ'_{aacc}	0.4782	Φ_{abb}	−0.372	d_2	0.000	h_1	0.005
	6	573.0	58.2	11.3	τ'_{bbcc}	−0.038	Φ_{aac}	−55.140			h_2	0.001
							Φ_{bbc}	0.019			h_3	0.000
							Φ_{acc}	0.132				
							Φ_{bcc}	0.009				
							Φ_{abc}	−1.446				
cis-HOCO	1	−682.5	−62.1	−59.3	τ'_{aaaa}	−10.445	Φ_{aaa}	255.528	D_J	0.017	H_J	−0.043
anion	2	207.3	10.6	8.2	τ'_{bbbb}	−0.088	Φ_{bbb}	−0.045	D_{JK}	0.039	H_{JK}	−2.704
	3	−28.9	56.9	74.3	τ'_{cccc}	−0.048	Φ_{ccc}	−0.044	D_K	2.556	H_{KJ}	–31.977
	4	−34.1	156.5	151.0	τ'_{aabb}	−0.278	Φ_{aab}	−20.902	d_1	−0.003	H_K	290.253
	6	428.2	138.7	125.4	τ'_{aacc}	−0.006	Φ_{abb}	−2.328	d_2	0.000	h_1	−0.001
	5	148.2	105.4	56.7	τ'_{bbcc}	−0.063	Φ_{aac}	−16.546			h_2	−0.001
							Φ_{bbc}	−0.083			h_3	0.000
							Φ_{acc}	−0.367				
							Φ_{bcc}	−0.075				
							Φ_{abc}	−3.342				

and combination band states, while the ν_4/ν_5 resonance could be considered a special example of a 1-1 resonance discussed in Ref. 53. Without this rare resonance specified, the CcCR ν_4 and ν_5 fundamentals computed by regular VPT theory (in the standard SPECTRO program) are 661.7 cm^{-1} and 534.5 cm^{-1}, which are 8.2 cm^{-1} lower and 9.9 cm^{-1} higher, respectively, than the VCI results. Including this resonance into our polyad treatment,[52] the discrepancies are dramatically reduced to 0.1 cm^{-1} and 1.8 cm^{-1}, i.e., back to the normal range of VPT/VCI agreements. We believe this improvement is *not* accidental. The ν_4 and ν_5 states in the VCI computation do show strong coupling between their CI basis, which have triggered the idea of including the ν_4/ν_5 resonance into VPT. This kind of resonance occurring between fundamentals may serve as a good example for a more accurate resonance testing scheme (see the Appendix of Ref. 52) by considering not only small denominators of the equations which give the anharmonicity constants, as is the current practice, but also big numerators, as well.

Additionally, there is very good agreement between VPT and VCI for the *cis*-HOCO anion. In fact, it is better than the predictions of the *cis*-HOCO radical above and the *trans*-HOCO radical previously.[18] All five of the a' modes have differences between VPT and VCI of less than 5 cm^{-1} except for the CR ν_2. Even so, this difference is just 5.2 cm^{-1}. Also, ν_4, the C−O_1 stretch, is nearly identical between the two approaches for a given QFF (666.5 and 666.4 cm^{-1} for CR VPT and VCI, respectively) as is the ν_1 O_1−H stretch for the CcCR QFF. The fact that the frequencies for the VPT and VCI CcCR ν_1 (3306.4 and 3306.5 cm^{-1}, respectively) and ν_4 modes (669.8 and 669.9 cm^{-1}, respectively) are nearly identical strengthens our prediction for the frequencies of these and even the other modes as two different methods closely corroborate the result for all the a' modes. The one obvious difference between VPT and VCI is in ν_6, the a" torsional mode. This same behavior has been observed for both conformers of the radical and, thus, this discrepancy in ν_6 may be an artifact of the computations where VCI can better treat the relatively large anharmonicity present in the torsional mode, whereas the perturbation approach of VPT cannot.

Interestingly, the difference between VPT and VCI is also consistent between the QFFs for the ν_6 mode even if the actual frequencies for choice of QFF are not identical. The VPT predicts a CcCR ν_6 frequency at 612.5 cm^{-1}, while VCI predicts this frequency at 598.0 cm^{-1}, a difference of 14.5 cm^{-1}. The CR QFF predicts a VPT frequency for ν_6 at 605.1 cm^{-1}, and 590.6 cm^{-1} is the frequency predicted by VCI. This difference is again 14.5 cm^{-1}. For the other modes, this difference is not quite as static, but the difference between VPT and VCI for the CR QFF is never more than about 1 cm^{-1} greater than this same difference for the CcCR QFF. The ν_1 mode is the most extreme example with a CcCR VPT/VCI difference of 0.2 cm^{-1} and a CR VPT/VCI difference of 1.8 cm^{-1}. Regardless, the consistency in the VPT/VCI difference for the choice of QFF demonstrates that VPT and VCI themselves are not further affected by the difference in terms from the composite energy and the subsequent force constants. This result also strengthens our predictions of the gas phase fundamental vibrational frequencies.

The choice of QFF does have some effect on the accuracy of the prediction for the frequencies of these modes, since the values differ by as much as 10 cm^{-1} in the case of ν_3 (1125.0 cm^{-1} for CcCR VCI and 1115.1 cm^{-1} for CR VCI). It is known that the removal of the core correlation effects in the prediction of fundamental vibrational frequencies does most prominently affect the bond lengths;[18,35] they are shorter (and more tightly bound thus giving higher frequencies) as showcased at the beginning of this section for comparison in the equilibrium geometries of the CcCR and CR QFFs. However, this results in more accurate predictions of the two known fundamental vibrational frequencies for the *trans*-HOCO radical compared to other, more descriptive QFFs.[54] This improved accuracy is probably the result of a cancellation of errors from the lack of inclusion of the higher order electron correlation terms. Even so, the previous evidence indicates that the CR QFF with its cancellation of errors is probably the more accurate result for the frequency of each mode. In spite of this, predictions of ν_1 are nearly identical using either QFF, and those for ν_4 exhibit only small differences. Hence, for most modes, either QFF will be a valid choice for the prediction of the fundamental vibrational frequencies of the *cis*-HOCO anion.

C. The $HOCO^-$ electron binding energy

Utilizing these QFFs, we can also offer insight into other properties that may assist in the experimental analysis of $HOCO^- \rightarrow HOCO + e^-$. Electron binding energies (eBEs) are a relevant property for any studies involving negatively charged molecular species, and adiabatic eBEs have been computed previously by some of us (R.C.F. and T.D.C.) in work relating to excited states of anions.[55,56] An eBE (also called an adiabatic electron affinity, AEA, in some studies) is simply the amount of energy required to retain the electron within the system.[57] Computationally, eBEs are the energy difference between the optimized structure of the radical and that of the anion.[58] Use of the CCSD(T)/aug-cc-pVTZ method and basis set in our previous studies report accuracies for adiabatic eBEs to better than 0.1 eV.[55,56]

For the *cis*-HOCO adiabatic eBE based on the *cis*-$HOCO^- \rightarrow$*cis*-HOCO + e^- formalism, our highly accurate CcCR QFF places the equilibrium adiabatic eBE for this system at 1.458 eV. For the more complete *cis*-$HOCO^- \rightarrow$ *trans*-HOCO + e^- description for the eBE where the more stable conformer of the HOCO radical is defined in the products, our computations from this study and those from our previous work[18] place the CcCR eBE at 1.380 eV. These two values are very close to 1.43 and 1.30 eV, respectively, eBEs previously computed with CCSD(T)/6-311++G(3*df*,3*pd*) by Clements *et al.*[1] and further verified experimentally by Lu and co-workers.[2,4] However, there was still uncertainty on the order of 0.3 eV between the previously predicted values and the experimental results where the necessary two-photon process was observed at 1.60 eV. Even though, our eBEs correct these initial computations by as much as 0.08 eV, another 0.22 eV discrepancy is present for the *cis*-$HOCO^- \rightarrow$*trans*-HOCO + e^- formalism of the eBE.

Additional uncertainty could be attributed to vibrational effects.[2] In these energy regimes, the 0.14 eV difference between our 1.458 eV eBE and the 1.60 eV eBE from experiment is 320 cm^{-1}, greater than the frequency of even the least energetic mode of the *cis*-HOCO anion or either of the radicals. Computing the zero-point corrected eBEs decreases the *cis*-$HOCO^- \rightarrow$ *trans*-HOCO + e^- CcCR eBE from 1.380 eV to 1.311 eV and the *cis*-$HOCO^- \rightarrow$ *cis*-HOCO + e^- CcCR eBE from 1.458 eV to 1.398 eV. These decreases are a product of the radicals having higher frequency modes than the anion. Subsequently, the decrease in the eBE for the zero-point correction results in a further move of the computed eBEs away from the best experimental value at 1.60 eV. Even so, the corroboration between the previous and the present computations coupled with the highly accurate geometries and fitting procedures utilized here all appear to indicate that the eBEs are well assigned for the HOCO anion into the two radical conformers.

IV. CONCLUSIONS

The computations carried out for the work reported here provide highly accurate gas phase fundamental vibrational frequencies for the $X\,^2A'$ *cis*-HOCO radical and the $X\,^1A'$ *cis*-HOCO anion. These two species are fundamentally related to one another in DPD experiments beginning with the anion and also in their relevance for the study of the HOCO radical in regards to the OH + CO atmospheric chemistry of the Earth, Mars, and, potentially, beyond. Through the use of QFFs computed with highly accurate *ab initio* methods, we utilized the same techniques previously used for the *trans*-HOCO radical,[18] where the fundamental frequencies were predicted to lie within 4 cm^{-1} of experimentally known values, for predictions of the fundamental vibrational frequencies and spectroscopic constants of both *cis*-HOCO systems.

For the computations of the fundamental frequencies, we made use of the VPT and VCI approaches, and the level of agreement between the two methods is striking. For all of the totally symmetric modes in both the anion and the radical, agreement between VPT and VCI is on the order of 5 cm^{-1} or less. Many states have agreement to better than 1 cm^{-1}. The difference between VPT and VCI for the a" torsional motion for both molecules is much larger, but this was also observed for the *trans*-HOCO radical.[18] The VCI procedure probably treats the energy of the torsional mode better than VPT. Hence, the relatively large anharmonicity of this mode may, again, require something beyond a QFF for its description. Additionally, the discrepancies in the frequencies between QFFs for both molecules of interest, though not ideal, is also good as it is on the order of 10 cm^{-1} or less. Since the CR QFF predicted the most accurate frequencies for the *trans*-radical conformer, we may also assume that its lower frequencies predicted for each mode are probably more accurate than the CcCR results. Regardless, the agreement between the VPT and VCI procedures as well as the good agreement between QFFs strengthens our predictions for the fundamental frequencies and the simultaneously computed spectroscopic constants of both the *cis*-HOCO radical and the *cis*-HOCO anion.

These full sets of fundamental vibrational frequencies are highly accurate gas phase values for these two molecules, and the first of such for the *cis*-HOCO anion. The agreement with previous theory in the prediction of geometrical parameters for both molecules as well as the closeness of the values for the zero-point structure of the radical to experiment, all to better than 1%, further strengthens our predictions. Our rotational constants also match previous theoretical predictions and experiment similarly well. Hence, the spectroscopic constants we report should assist in microwave studies and interstellar observations of these systems. Finally, we provide highly accurate corroborating evidence for previous predictions of electron binding energies relevant to the DPD experiments of $HOCO^-$.

In the pursuit of further understanding of chemistry as fundamental as the reaction of OH + CO, the spectroscopic constants and fundamental vibrational frequencies of the HOCO radical and anion are essential. We provide theoretical predictions of these data in order to help elucidate the processes related to this reaction both for application to our own atmosphere and also to those planetary envelopes which are yet to be explored.

ACKNOWLEDGMENTS

The work undertaken by R.C.F. and T.D.C. is supported by the U.S. National Science Foundation through award CHE-1058420 and through a Multi-User Chemistry Research Instrumentation and Facility (CRIF:MU) award CHE-0741927. T.J.L. and X.H. gratefully acknowledge funding from NASA Grant No. 08-APRA08-0050 and NASA Grant No. 10-APRA10-0096. X.H. also acknowledges support from the NASA/SETI Institute Cooperative Agreement NNX09AI49A. Dr. Andrew Simmonett of the University of Georgia once more allowed us to use his CheMVP program in the creation of Fig. 1.

[1] T. G. Clements, R. E. Continetti, and J. S. Francisco, J. Chem. Phys. **117**, 6478 (2002).
[2] Z. Lu, J. E. Oakman, and R. E. Continetti, J. Chem. Phys. **126**, 194305 (2007).
[3] Z. Lu and R. E. Continetti, Phys. Rev. Lett. **99**, 113005 (2007).
[4] Z. Lu, J. E. Oakman, Q. Hu, and R. E. Continetti, Mol. Phys. **106**, 595 (2008).
[5] D. E. Milligan and M. E. Jacox, J. Chem. Phys. **54**, 927 (1971).
[6] I. W. M. Smith and R. Zellner, J. Chem. Soc. Faraday Trans. **69**, 1617 (1973).
[7] J. S. Francisco, J. T. Muckerman, and H.-G. Yu, Acc. Chem. Res. **43**, 1519 (2010).
[8] J. Barker and D. Golden, Chem. Rev. **103**, 4577 (2003).
[9] R. A. Marcus, "Applications of theoretical methods to atmospheric sciences," in *Advances in Quantum Chemistry* (Elsevier, Amsterdam, 2008), Vol. 55, pp. 5–19.
[10] S. K. Atreya and Z. G. Gu, J. Geophys. Res., [Planets] **99**, 13133 (1994).
[11] K. Zahnle, R. M. Haberle, D. C. Catling, and J. F. Kasting, J. Geophys. Res., [Planets] **113**, E11004 (2008).
[12] G. A. Soffen, Science **194**, 1274 (1976).
[13] H. Yu, J. Muckerman, and T. Sears, Chem. Phys. Lett. **349**, 547 (2001).
[14] T. J. Sears, W. M. Fawzy, and P. M. Johnson, J. Chem. Phys. **97**, 3996 (1992).
[15] J. T. Petty and C. B. Moore, J. Mol. Spectrosc. **161**, 149 (1993).
[16] M. E. Jacox, J. Chem. Phys. **88**, 4598 (1988).
[17] D. Forney, M. E. Jacox, and W. E. Thompson, J. Chem. Phys. **119**, 10814 (2003).

[18]R. C. Fortenberry, X. Huang, J. S. Francisco, T. D. Crawford, and T. J. Lee, J. Chem. Phys. **135**, 134301 (2011).
[19]C. E. Dateo, T. J. Lee, and D. W. Schwenke, J. Chem. Phys. **101**, 5853 (1994).
[20]T. J. Lee, J. M. L. Martin, and P. R. Taylor, J. Chem. Phys. **102**, 254 (1995).
[21]X. Huang and T. J. Lee, J. Chem. Phys. **129**, 044312 (2008).
[22]X. Huang and T. J. Lee, J. Chem. Phys. **131**, 104301 (2009).
[23]X. Huang, P. R. Taylor, and T. J. Lee, J. Phys. Chem. A **115**, 5005 (2011).
[24]T. J. Lee and G. E. Scuseria, in *Quantum Mechanical Electronic Structure Calculations with Chemical Accuracy*, edited by S. R. Langhoff (Kluwer Academic Publishers, Dordrecht, 1995), pp. 47–108.
[25]T. D. Crawford and H. F. Schaefer, in *Reviews in Computational Chemistry*, edited by K. B. Lipkowitz and D. B. Boyd (Wiley, New York, 2000), Vol. 14, pp. 33–136.
[26]T. Helgaker, T. A. Ruden, P. Jørgensen, J. Olsen, and W. Klopper, J. Phys. Org. Chem. **17**, 913 (2004).
[27]A. P. Rendell, T. J. Lee, and P. R. Taylor, J. Chem. Phys. **92**, 7050 (1990).
[28]K. Raghavachari, G. W. Trucks, J. A. Pople, and M. Head-Gordon, Chem. Phys. Lett. **157**, 479 (1989).
[29]J. D. Watts, J. Gauss, and R. J. Bartlett, J. Chem. Phys. **98**, 8718 (1993).
[30]A. C. Scheiner, G. E. Scuseria, J. E. Rice, T. J. Lee, and H. F. Schaefer III, J. Chem. Phys. **87**, 5361 (1987).
[31]G. E. Scuseria, J. Chem. Phys. **94**, 442 (1991).
[32]T. H. Dunning, J. Chem. Phys. **90**, 1007 (1989).
[33]K. A. Peterson and T. H. Dunning, J. Chem. Phys. **102**, 2032 (1995).
[34]R. A. Kendall, T. H. Dunning, and R. J. Harrison, J. Chem. Phys. **96**, 6796 (1992).
[35]J. M. L. Martin and P. R. Taylor, Chem. Phys. Lett. **225**, 473 (1994).
[36]J. M. L. Martin and T. J. Lee, Chem. Phys. Lett. **258**, 136 (1996).
[37]M. Douglas and N. Kroll, Ann. Phys. **82**, 89 (1974).
[38]X. Huang, D. W. Schwenke, and T. J. Lee, J. Chem. Phys. **129**, 214304 (2008).
[39]H.-J. Werner, P. J. Knowles, F. R. Manby, M. Schütz, *et al.*, MOLPRO, version 2010.1, a package of *ab initio* programs, 2010, see http://www.molpro.net.
[40]INTDER 2005 is a general program written by W. D. Allen and co-workers, which performs vibrational analysis and higher order nonlinear transformations, 2005.
[41]I. M. Mills, in *Molecular Spectroscopy – Modern Research*, edited by K. N. Rao and C. W. Mathews (Academic, New York, 1972).
[42]J. K. G. Watson, in *Vibrational Spectra and Structure*, edited by J. R. During (Elsevier, Amsterdam, 1977).
[43]D. Papousek and M. R. Aliev, *Molecular Vibration-Rotation Spectra* (Elsevier, Amsterdam, 1982).
[44]J. F. Gaw, A. Willets, W. H. Green, and N. C. Handy, SPECTRO program, version 3.0, 1996.
[45]S. Carter, J. M. Bowman, and N. C. Handy, Theor. Chem. Acc. **100**, 191 (1998).
[46]J. M. Bowman, S. Carter, and X. Huang, Int. Rev. Phys. Chem. **22**, 533 (2003).
[47]T. Oyama, W. Funato, Y. Sumiyoshi, and Y. Endo, J. Chem. Phys. **134**, 174303 (2011).
[48]P. Botschwina, Mol. Phys. **103**, 1441 (2005).
[49]D. Dixon, D. Feller, and J. Francisco, J. Phys. Chem. A **107**, 186 (2003).
[50]J. M. Bowman, K. Christoffel, and G. Weinberg, J. Mol. Struct. **461**, 71 (1999).
[51]G. C. Shatz, M. S. Fitzcharles, and L. B. Harding, Faraday Discuss. Chem. Soc. **84**, 359 (1987).
[52]J. M. L. Martin, T. J. Lee, P. R. Taylor, and J.-P. François, J. Chem. Phys. **103**, 2589 (1995).
[53]J. M. L. Martin and P. R. Taylor, Spectrochim. Acta, Part A **53**, 1039 (1997).
[54]Even though the CcCR QFF contains more terms describing the energy at each point on the potential surface, Ref. 18 reports that the CR QFF ν_1 and ν_2 fundamental frequencies are closer to the known experimental values for these modes than the CcCR or even the CcCRE results.
[55]R. C. Fortenberry and T. D. Crawford, J. Chem. Phys. **134**, 154304 (2011).
[56]R. C. Fortenberry and T. D. Crawford, J. Phys. Chem. A **115**, 8119 (2011).
[57]J. Simons, J. Phys. Chem. A **112**, 6401 (2008).
[58]J. Simons, Annu. Rev. Phys. Chem. **62**, 107 (2011).